Growth of Microscale In_2O_3 Islands on Y-Stabilized Zirconia(100) by Molecular Beam Epitaxy

A. Bourlange,[†] D. J. Payne,[†] R. M. J. Jacobs,[†] R. G. Egdell,*[,†] J. S. Foord,[†] A. Schertel,[‡] P. J. Dobson,[§] and J. L. Hutchison[||]

Department of Chemistry, Chemistry Research Laboratory, University of Oxford, Mansfield Road, Oxford OX1 3TA, United Kingdom, Carl Zeiss SMT AG, Carl-Zeiss-Strasse 56, 73447 Oberkochen, Germany, Oxford University Begbroke Science Park, Sandy Lane, Yarnton, Kidlington, Oxon OX5 1PF, United Kingdom, and Department of Materials, University of Oxford, Parks Road, Oxford OX1 3PH, United Kingdom

Received April 7, 2008

Mismatch between the lattice parameters for a substrate and an epilayer deposited by molecular beam epitaxy (MBE) can promote the development of self-assembled "dot" structures, usually on a nanometer length scale. To date most work in this area has concentrated on quantum dots obtained in the hetero epitaxial growth of III−V semiconductors, typified by InAs on GaAs where there is a 7% lattice mismatch.[1–3] In the present communication we extend this approach to the growth of micrometer sized arrays of In_2O_3 islands on Y-stabilized ZrO_2(100).

In_2O_3 is an n-type oxide amenable to degenerate n-type doping to give a material which combines optical transparency in the visible region with a high conductivity. This leads to important applications in liquid crystal displays, solar cells, and electroluminescent display devices.[4] We have very recently shown that continuous epitaxial films of In_2O_3 can be grown on (100) oriented yttria-stabilized zirconia substrates at a temperature of 650 °C.[5] ZrO_2 itself has a low symmetry monoclinic structure at room temperature, but a cubic phase can be stabilized by replacement of Zr(IV) with larger cations such as Ca(II) or Y(III) and with concomitant introduction of compensating oxygen vacancies. The lattice parameter of the face centered cubic fluorite phase increases with Y doping level. For the minimum Y concentration of around 17% required to stabilize the cubic phase the lattice parameter $a = 5.1423$ Å, while for 28% Y-doping $a = 5.2100$ Å. The body centered bixbyite structure of In_2O_3 has $a = 10.1170$ Å and is derived from a $2 \times 2 \times 2$ superstructure of the fluorite structure with one-fourth of the anion sites vacant. Thus at 17% Y-doping there is a mismatch of 1.6% between $2a$ for Y-ZrO_2 and a for In_2O_3, increasing to 3.0% at 28% Y doping.[6,7] For this reason yttria stabilized zirconia has been proven to be one of the most popular substrates for attempted epitaxial growth of In_2O_3.[8–11] In the present communication it is shown that MBE growth of In_2O_3 at high temperatures (typically around 900 °C) on cubic ZrO_2 stabilized by 17% Y-doping promotes break-up of the continuous films obtained at lower temperatures into striking arrays of highly oriented truncated square pyramidal *micrometer* sized epitaxial islands with a narrow size distribution. The edges of the islands are uniformly aligned parallel to ⟨110⟩ directions of the substrate and display a narrow size distribution. This unanticipated growth mode is apparently driven by the small mismatch between the intercation separations in the two oxides and a propensity for development of (111) side facets on the islands.

Indium oxide layers were grown on Y-stabilized ZrO_2(100) substrates (PiKem, U.K.) in a an UHV oxide MBE system (SVT, U.S.A.) system with a base pressure of 5×10^{-10} mbar and incorporating an indium Knudsen cell and a radiofrequency oxygen plasma source, as described in detail elsewhere.[5] Substrates were cleaned by exposure to the oxygen atom beam at a substrate temperature of 900 °C. Films were then grown to an estimated thickness of 120 nm with a deposition rate of 0.04 nm/s at a substrate temperature of 900 °C. AFM images were recorded in a Digital Instruments Multimode SPM instrument with a Nanoscope IIIa controller. This was operated in tapping mode with an "J" scanner having a lateral range of approximately 100 μm and a vertical range of 6 μm. Silicon probes (Nascatec GmbH model NST NCHFR), with resonant frequencies of approximately 320 kHz. Calibration of the AFM was accomplished by scanning a 10 μm pitch 200 nm 3D reference from Digital instruments. Thin lamellar slices for analysis by high resolution transmission electron microscopy were prepared in a Zeiss NVision 40 focused ion beam (FIB) instrument incorporating a Ga liquid metal ion source and in situ SEM imaging using a thermal field emission source.[5] HRTEM observations were carried out using a JEOL 4000EX microscope operating at 400 kV.

Figure 1a shows a large area AFM image of a typical film grown at 900 °C. The surface is covered by a striking array of islands with a square shape. Island growth is also obvious from X-ray photoelectron spectra (not shown) which contain strong Y and Zr core peaks characteristic of the substrate even when the nominal film thickness (assuming a continuous growth mode) is in excess of 100 nm. From the known bulk crystallographic directions of the substrate we may infer that the islands are all oriented with edges parallel to the

[†] Department of Chemistry, University of Oxford.
[‡] Carl Zeiss.
[§] Oxford University Begbroke Science Park.
[||] Department of Materials, University of Oxford.

(1) Schaffer, W. J.; Lind, M. D.; Kowalczyk, S. P.; Grant, R. W. *J. Vac. Sci. Technol., B* **1983**, *1*, 688.
(2) Yoffe, A. D. *Adv. Phys.* **2001**, *50*, 1.
(3) Marzi, J. Y.; Gerard, J. M.; Izrael, A.; Barrie, D.; Bastard, G. *Phys. Rev. Lett.* **1994**, *73*, 716.
(4) Granqvist, C. G. *Sol. Energy Mater. Sol. Cells* **2007**, *91*, 1529.
(5) Bourlange, A.; Payne, D. J.; Egdell, R. G.; Foord, J. S.; Edwards, P. P.; Jones, M. O.; Schertel, A.; Dobson, P. J.; Hutchison, J. L. *Appl. Phys. Lett.* **2008**, *92*, 092117.
(6) Moringa, M.; Cohen, J. B. *Acta Crystallogr., Sect. A* **1979**, *35*, 789.
(7) Horiuchi, H.; Schultz, A. J.; Leung, P. C.; Williams, J. M. *Acta Crystallogr., Sect. B* **1984**, *40*, 367.
(8) Ohta, H.; Orita, M.; Hirano, M.; Tanji, H.; Kawazoe, H.; Hosono, H. *Appl. Phys. Lett.* **2000**, *76*, 2740.
(9) Ohta, H.; Orita, M.; Hirano, M.; Hosono, H. *J. Appl. Phys.* **2002**, *91*, 3547.
(10) Koida, T.; Kondo, M. *J. Appl. Phys.* **2006**, *99*, 123703.
(11) Taga, N.; Maekwa, M.; Shigesato, Y.; Yasui, I.; Kakei, M.; Haynes, T. E. *Jpn. J. Appl. Phys.* **1998**, *37*, 6524.

10.1021/cm800984r CCC: $40.75
Published on Web 06/28/2008

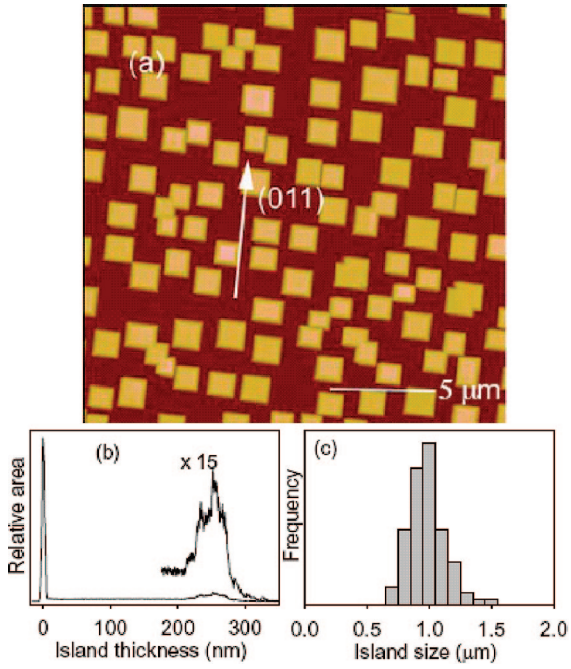

Figure 1. (a) AFM (20 μm × 20 μm) image of the of In_2O_3 islands on Y-stabilized ZrO_2. (b) Bearing analysis of height distribution of the image in (a). (c) Histogram of lateral sizes of the islands in (a)

⟨110⟩ directions of the Y-stabilized ZrO_2. The dimensions of the islands were found from the AFM images. A Bearing analysis (Figure 1b) allowed the distribution of surface heights of the sample to be determined and revealed the islands to be 250 ± 40 nm thick. The mean surface area of the islands was determined to be 1.03 ± 0.33 μm^2, corresponding to a mean lateral side length of around 1.01 ± 0.16 μm (Figure 1c). AFM deflection images suggest that the islands have sloping facetted sides, and this is confirmed by scanning electron microscopy (SEM), as shown in Figures 2a,b and transmission electron microscopy (Figures 2c). The facets mostly had (111) surfaces, but occasionally higher index (211) facets were found as is shown in Figure 2c. For the fluorite structure the (100) and (111) surfaces are polar, whereas (110) is a nonpolar surface and is therefore expected to have a lower surface energy. Thus an island orientation which promotes development of (111) rather than (110) side facets is surprising, although it must be recognized that fluorite and bixbyite structures are not identical. Moreover the appearance of (111) facets is consistent with the observation that $\Delta\omega$ rocking curve widths are much smaller for In_2O_3 grown on Y-stabilized ZrO_2(111) than on (100) substrates,[9] suggesting that In_2O_3(111) has a low surface energy.

The epitaxial relationship between the In_2O_3 islands and the substrate is confirmed by selected area electron diffraction carried out in the HRTEM. Lamellar slices were cut from the sample shown in Figure 1 both parallel to and at 45° to the island edges, corresponding to ⟨110⟩ and ⟨100⟩ directions of the substrate. Figure 3 shows electron diffraction patterns from these slices taken down the ⟨110⟩ and ⟨100⟩ directions for both the Y-ZrO_2 (parts a and c of Figure 3, respectively) and for the In_2O_3 epilayer (parts b and d of Figure 3, respectively). The diffraction patterns firmly establish the azimuthal orientation of the islands relative to the substrate

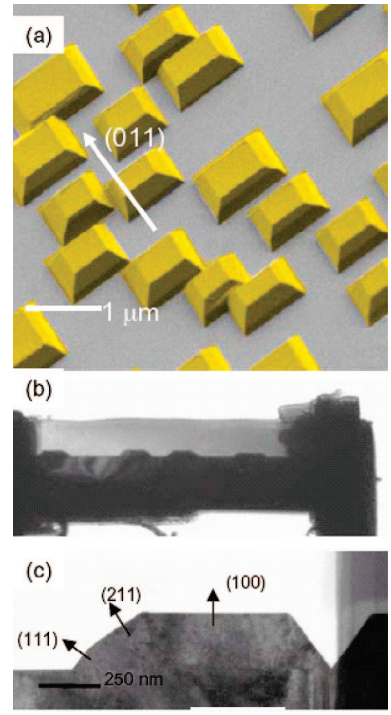

Figure 2. (a) Secondary electron SEM image of In_2O_3 islands taken in the FIB system with a 1.5 kV electron beam. The islands are enhanced in false color. The image appears foreshortened as it is taken at 45° to the sample surface down the (011) direction. (b) Cross sectional image of a lamellar slice showing several islands, also taken in the FIB system. (c) Cross sectional image of an individual island taken in the HRTEM system.

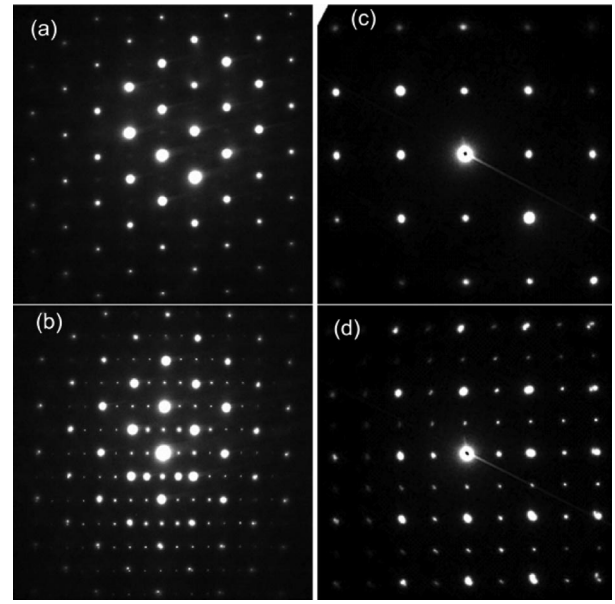

Figure 3. Selected area electron diffraction patterns from two different lamellar slices. (a) Y-doped ZrO_2 substrate down ⟨110⟩, (b) In_2O_3 epilayer down ⟨110⟩, (c) Y-doped ZrO_2 substrate down ⟨100⟩, and (d) In_2O_3 epilayer down ⟨100⟩.

and clearly reveal the doubling of the lattice parameter of the In_2O_3 epilayer relative to that of the substrate expected on the basis of the crystal structures. There are also indications of a small tilting of the epilayer relative to the substrate, which is about 2.5° in the ⟨100⟩ projection. High resolution lattice images are shown in Figure 4 viewed down ⟨110⟩ and ⟨100⟩ directions. The HRTEM images reveal abrupt but not completely smooth interfaces between the

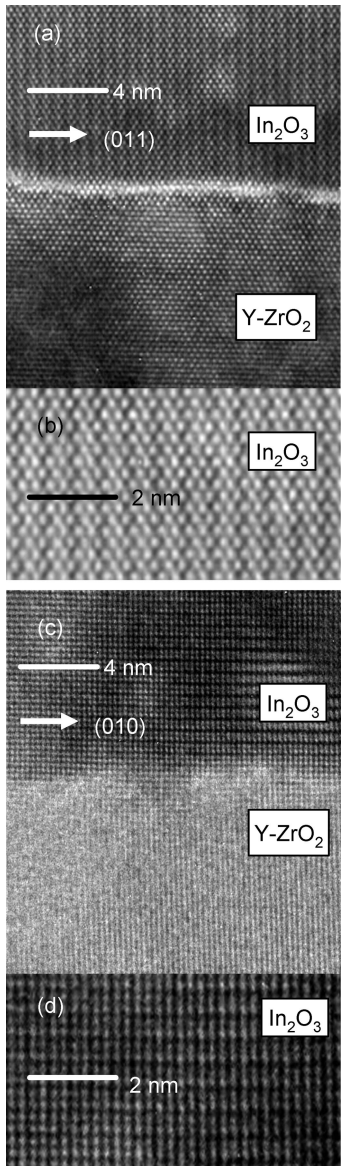

Figure 4. HRTEM images of the In_2O_3/Y-ZrO_2 interface viewed in (a) ⟨110⟩ and (b) ⟨100⟩ projections. Expanded images of the epilayer in the two projections are shown in (c) and (d).

island epilayers and the substrate and confirm the excellent epitaxial registry between the two.

There is a growing interest in the use of large quantum III−V dots as detectors for THz radiation or as THz oscillators.[12–14]

Consider the following very simple argument. For an electron gas confined to a box of side L the separation δE between energy levels at the Fermi level is

$$\delta E = \frac{\hbar^2}{m^*} k_F \delta k$$

where m^* is the electron effective mass, $\delta k = \pi/L$, and k_F is the wavenumber at the Fermi level. The layers of In_2O_3 we grow by MBE typically have free electron carrier concentrations of around 10^{20} cm^{-3} due to n-type doping associated with oxygen vacancy defects.[5] Taking $m^* = 0.35m_0$ (where m_0 is the electron rest mass)[15] it follows that lateral confinement with $L = 1$ μm gives $\delta E = 1$ meV, corresponding to a frequency of about 0.25 THz. The confinement normal to the surface where $L = 250$ nm will lead to quantization on an energy scale of order 4 meV, corresponding to a frequency of about 1.0 THz. The effects of quantum confinement will however only be observable if the electron mean free path exceeds the box size. The THz absorption properties of our island films are currently under investigation, although the substrate itself shows pronounced absorption in the terahertz regime.

In summary we have developed a procedure for growth of islands of In_2O_3 on Y-stabilized ZrO_2 with a uniform azimuthal orientation and with a narrow size distribution. Y-stabilized ZrO_2 is a versatile substrate whose lattice parameter varies with Y doping level, thus providing a means of varying the mismatch with In_2O_3 epilayers and a means to control the island size.

Acknowledgment. This work was supported by EPSRC Grant GRS/94148.

CM800984R

(12) Metzner, C.; Stehr, D. *Phys. Rev. B* **2004**, *70*, 195433.
(13) Vurgraftman, I.; Meyer, J. R.; Wu, D. H.; Bussman, K.; Jonker, B. T. *J. Appl. Phys.* **2006**, *100*, 064509.
(14) Hashiba, H.; Das, B.; n/a, B.; Nicholls, J. T.; Antonov, V.; Kulik, L.; Komiyama, K. *Physica E* **2006**, *34*, 644.
(15) Hamberg, I.; Granqvist, C. G.; Berggren, K. F.; Sernelius, B. E.; Egström, L. *Phys. Rev. B* **1984**, *30*, 3240.